Mechanotransduction in Lateral Root Initiation: A Model Integrating Growth Mechanics and Auxin Signaling

João R. D. Ramos[1], Blanca Jazmin Reyes-Hernández[2], Karen Alim[1,✉], and Alexis Maizel[2,✉]

[1]Technical University of Munich, Germany; TUM School of Natural Sciences, Department of Bioscience; Center for Protein Assemblies (CPA)
[2]Center for Organismal Studies (COS), Univrsity of Heidelberg, Im Neuenheimer Feld 230, 69120 Heidelberg, Germany

Plant development relies on the precise coordination of cell growth, which is influenced by the mechanical constraints imposed by rigid cell walls. The hormone auxin plays a crucial role in regulating this growth by altering the mechanical properties of cell walls. During the post-embryonic formation of lateral roots, pericycle cells deep within the main root are triggered by auxin to resume growth and divide to form a new root. This growth involves a complex interplay between auxin, growth, and the resolution of mechanical conflicts. However, the exact mechanisms by which this coordination is achieved are still unknown. Here, we propose a model that integrates tissue mechanics and auxin transport, revealing a connection between the auxin-induced relaxation of mechanical stress in the pericycle and auxin signalling in the endodermis. We show that the growth of pericycle cells is initially limited by the endodermis, resulting in a modest initial growth. However, this modest growth is sufficient to redirect auxin to the overlying endodermis, which then actively accommodates the growth, allowing for the subsequent development of the lateral root. Our model uncovers the mechanical parameters that underlie endodermal accommodation and how the structure and shape of the endodermis influence the formation of the new root. These findings highlight the interconnected relationship between mechanics and auxin flow during lateral root initiation, emphasizing the vital role of the endodermis in shaping root development through mechanotransduction and auxin signalling.

Plant Development | Intercellular Coordination | Auxin Signaling | Mechanical Feedback | Lateral Root Initiation

Correspondence: ***alexis.maizel@cos.uni-heidelberg.de; k.alim@tum.de***

Introduction

The rigidity of plant cell walls imposes precise coordination of growth among cells, where spatial variations in growth generate mechanical stresses serving as instructive cues. This feedback mechanism links tissue geometry to gene expression (1, 2). Auxin, a pivotal plant hormone involved in cell growth and differentiation (3–9), plays a central role in growth regulation by modifying cell wall properties (10, 11). Its distribution relies on polar transport regulated by influx and efflux carriers (12–14). Efflux carrier polarization, particularly the PIN protein family, directs auxin flow, regulating plant growth and development (15–17). PIN proteins have also been found to possess mechanical-sensing properties (18, 19), contributing to the complex interplay between auxin-mediated cell wall softening, tissue mechanics, and PIN-mediated auxin transport, ultimately shaping developmental auxin patterns (18, 20).

A prime example of coordinated cell and tissue growth is the formation of lateral roots (LRs) (21–23). In *Arabidopsis thaliana*, LRs originate from pericycle cells beneath the endodermis (24, 25). These Xylem pole pericycle (XPP) cells, typically in pairs, become activated through auxin accumulation, driven by local synthesis (26), lateral auxin diversion (27–29), and endodermal-to-pericycle auxin reflux (30) (Fig. 1 A). Activated XPP cells expand radially, pressing against the overlying endodermis (31). Nuclei migrate, triggering asymmetric cell division and lateral root primordium formation (21, 23, 32). Notably, this radial expansion is more pronounced at shared cell walls (31, 33), necessitating cortical microtubule (CMT) rearrangements in founder cells (33). Endodermis shape changes and LR initiation depends on auxin signalling in the endodermis (31, 34) and a reversion in auxin flow from the pericycle toward the endodermis (30, 31). Several questions needs to be addressed to understand the dramatic mechanical changes associated with LR initiation. In particular, how do mechanics and growth interact with auxin flows? What mechanical properties of the tissue need to change to allow swelling of the founder cells? What can we explain the presence of auxin in the endodermis?

Here, we use a model to examine the interplay between growth mechanics and auxin flow during LR initiation. Our model combines a vertex model for tissue mechanics and a compartment model for auxin transport (20). We find that the shared anticlinal wall's growth between adjacent XPP cells is constrained, inducing only modest radial swelling. However, stress relaxation in this wall relocates auxin efflux carriers to the periclinal walls, redirecting auxin flow to the endodermis, and triggering an auxin-dependent response. Empirical observations support this prediction. Furthermore, we demonstrate that endodermal wall properties and arrangement predominantly limit the radial expansion of activated XPP cells. These findings propose a biphasic radial growth model for activated XPP cells, initially constrained by the endodermis, enabling auxin redirection to the endodermis. This, in turn, triggers an auxin-dependent response, facilitating radial expansion of activated XPP cells.

DRAFT

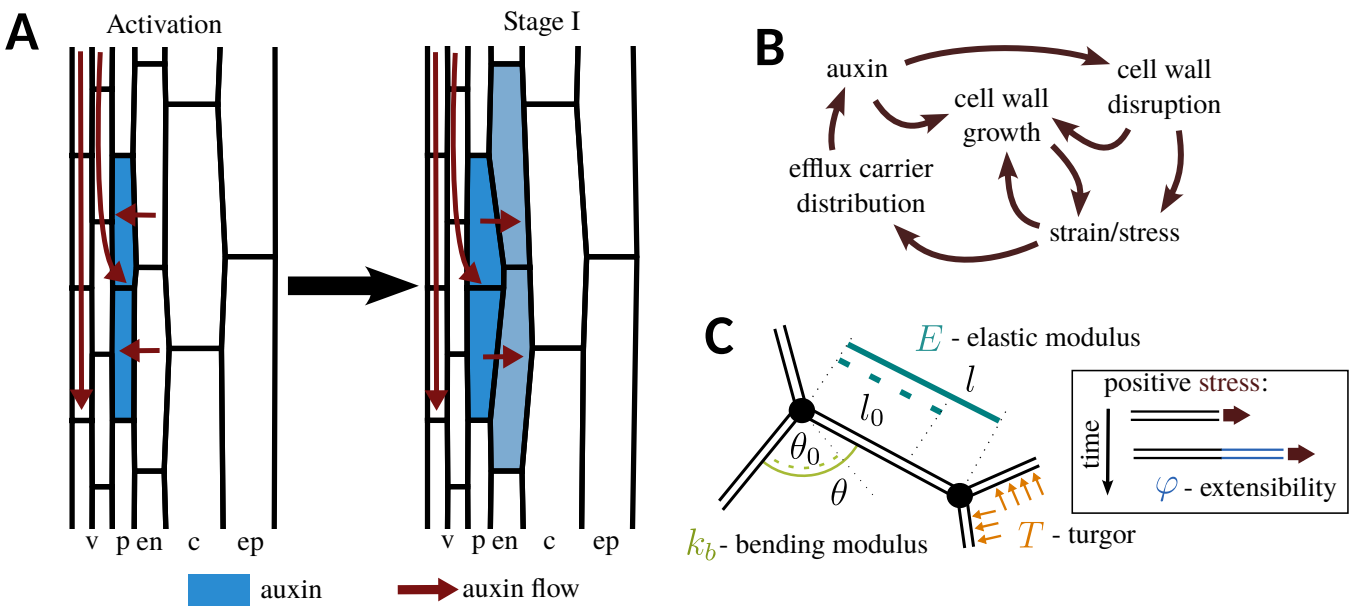

Fig. 1. Biological context and modelling framework (A) Activation of pericycle (p) before lateral root initiation results from the accumulation of auxin in these cells by local auxin synthesis, redirection of the rootward auxin flow in the vasculature (v) and from the endodermis (en). Upon activation, the pericycle cells with high auxin acquire a trapezoidal shape, and the endodermis accommodates this morphological change by shrinking, culminating in a stage I primordium. This accommodation of the endodermis requires auxin accumulation in the endodermis and its perception by *SHY2*. The diagram visualises the cellular template used in our mechanical vertex model, including the cortex (c) and epidermis (ep). (B) The interplay between auxin accumulation and cell wall mechanics. Auxin induces growth by altering the properties of the cell wall, which modifies the patterns of mechanical stress. Efflux carriers of auxin respond to mechanical perturbations, creating a mechanical feedback loop that affects the pattern of auxin concentration and flow. (C) In our model, cell walls are modelled as viscous rods that resist longitudinal deformations with an elastic modulus, E, and bending at the junctions with bending modulus k_b. Turgor, T, generates stresses to which the walls respond by growing according to their extensibility, φ.

Results and discussion

Model and assumptions. We previously developed a comprehensive two-dimensional vertex model that integrates a compartmental model for auxin transport to explore the interaction between tissue mechanics and auxin patterns (20). In this model, hexagonal cells subject to hydrostatic pressure exhibit resistance to compression, extension, and bending at their junctions (Fig. 1 C). The model accounts for auxin synthesis, degradation, and active/passive transport across cell walls. Auxin concentration within each cell is regulated by synthesis, influx, and efflux carriers, with efflux carriers responding to membrane stress. Higher wall stress increases efflux carrier accumulation, facilitating auxin transport up the concentration gradient (20).

To study the interplay between tissue mechanics and auxin flow during lateral root initiation, we adapted our model. We adjusted the cellular templates to match *in vivo* aspect ratios using optical longitudinal sections of *Arabidopsis thaliana* roots, resulting in six cell layers representing vasculature, pericycle cells, endodermis, cortex, and epidermis (Fig.1 A). Additionally, we incorporated cell wall growth into the model, representing cell walls as viscoelastic materials with an extensibility parameter (φ) and elastic modulus (E), determining wall expansion rate and response to longitudinal stress, respectively. Cell walls also resist bending at junctions governed by the bending modulus (k_b) (Fig.1 C). Cell-specific mechanical properties were considered between adjacent cells, with two compartments having distinct E and φ values. The model accounted for the less extensible compartment's constraint on cell wall growth, favouring growth when the combined wall resides between cells of higher extensibility (φ). Accumulation of auxin in root pericycle cells specifies them as lateral root founder cells (24). Our model incorporates two neighbouring pericycle cells, each with double the auxin concentration of surrounding cells, reflecting the initiation process (32).

Auxin accumulation in activated XPP cells leads to modest radial growth and redirects auxin flows towards endodermis. We first examined how an increase in auxin concentration alone contributes to the radial expansion of a pair of founder cells during lateral root initiation. To quantify this expansion, we tracked changes in the length of the shared interface between the two activated XPP cells and their overall morphology. Our simulations showed that growth occurs but rapidly saturates at around a 12% increase (Fig. 2 A). This growth coincides with reduced stress within the common wall (Fig. 2 B). However, the overall cell shape remains distinct from the trapezoidal configuration characteristic of activated XPP cells preparing for asymmetric division (Fig. 2 C).

As stress diminishes within the shared wall connecting the two activated XPP cells, the density of auxin efflux carriers binding to this interface decreases. In our model, carriers compete for binding among different interfaces, leading to the migration of carriers to the next most stressed interface. Initially, the highest density of auxin efflux carriers is in the anticlinal wall between the adjacent activated XPP cells (Fig. S1 A). With growth and stress reduction, carrier density increases, particularly binding toward the endodermis (Fig. S1 B). Notably, even though the efflux carrier density associated with the endodermis remains relatively low,

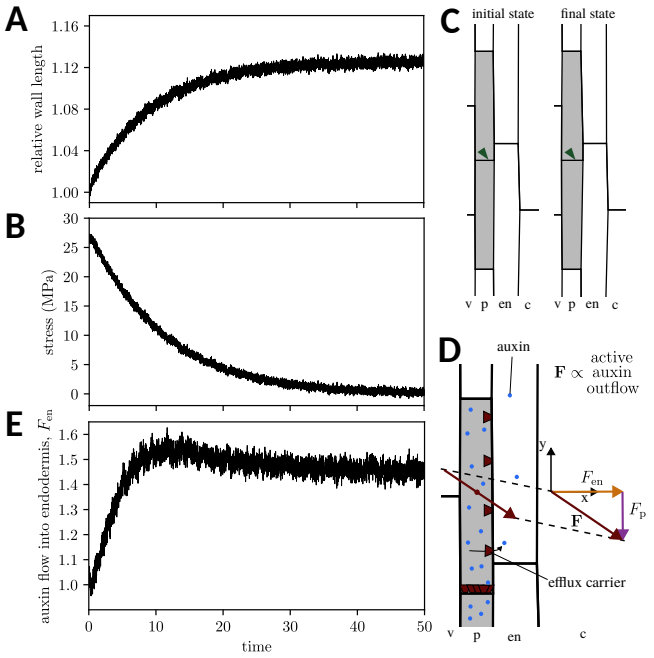

Fig. 2. Auxin accumulation in activated XPP cells only triggers modest growth but potentiates auxin flows towards the endodermis. (A) The relative length of the shared wall (green arrowheads in C) between two activated XPP cells (grey cells) increases over time, reaching a saturation value of around 12%. Accompanying this growth, stress decreases over time (B). The final state of the tissue remains geometrically close to the initial one (C). (D) Computation of the auxin flow. Integrating the density of auxin efflux carriers along the length of the activated XPP cells determines the flow of auxin leaving the cell (F). This vector can be decomposed in one component toward the endodermis (F_{en}) and one parallel to the pericycle layer (F_{p}). (E) The relative intensity of auxin flow leaving the activated XPP cell toward the endodermis (F_{en}). In (A), (B) and (E), the measures are normalised to the value at $t = 0$ (initial state). $t = 50$ marks the final state. The different layers are labelled: vasculature (v), pericycle (p), endodermis (en), cortex (c).

the cross-sectional area through which auxin flows must be considered. We introduce a measure similar to the polarity concept in (20) to quantify auxin flow due to auxin efflux carriers, showing how the component of auxin flow directed toward the endodermis evolves over time (Fig. 2 D, E). This measure is directly proportional to the net outflow of auxin (Supporting Information Eq. 13). With auxin-induced stress relaxation between adjacent cells, a 40-50% increase in auxin flow exiting the cell toward the endodermis is predicted.

It's important to note that these findings depend on the selected periclinal stress value. Since efflux carriers prefer binding to anticlinal walls (25), we chose a lower periclinal wall stress value, approximately $\sigma = 20\,\text{MPa}$. This choice was made to align the initial rest lengths of periclinal walls with the desired overall stress value of a periclinal wall. Selecting a very low stress value would obstruct efflux-mediated auxin transport between different layers.

In summary, our results indicate that increased auxin concentration within adjacent pericycle cells can induce softening of the shared anticlinal wall, resulting in a modest expansion that alone falls short of reproducing the typical cell aspect changes observed *in vivo*. Nevertheless, our model predicts that this stress-induced alteration in auxin efflux carriers subsequently triggers a redistribution, leading to a 40-50% enhancement in auxin flow from the founder cells toward the endodermis.

Auxin signaling in the endodermis predates the activation of SHY2 expression and the pronounced radial expansion of the activated pericycle. Increased auxin flow toward the endodermis, where it may trigger auxin accumulation, acting as a signal. This suggests that auxin responses should first occur in activated XPP cells and then in the endodermis (31). *SHY2* encodes an AUX/IAA involved in endodermal auxin perception and subsequent endodermal remodelling (31). Controlled transcriptionally by auxin (35), a *SHY2* reporter shows endodermal expression from Stage I onwards (31). To empirically verify that endodermal response to auxin, followed by activation of *SHY2*, is happening after redirection of auxin flow from the activated XPP cells, we live-imaged the expression of the nuclear auxin signalling output *DR5v2::Venus* (36) and the *SHY2* transcriptional reporter (31).

Before pericycle activation, neither *SHY2* nor *DR5v2* expression was observed in pericycle or endodermis. Upon activation, *DR5v2* signal appeared in pericycle and contiguous endodermal layers, while *SHY2* expression was solely in pericycle (Fig. 3 A). At Stage I, coinciding with noticeable pericycle swelling (Fig. 3 B), *SHY2* and *DR5v2* were observed in both pericycle and endodermis. This sequential auxin signalling in the endodermis, followed by *SHY2* activation, is in agreement with previous observations (30) and supports the model's prediction that reversed auxin flow due to modest pericycle expansion can initiate endodermal auxin responses (31).

Our model predicts that auxin accumulation within founder cells induces stress relaxation in the shared anticlinal wall, redirecting auxin flow toward the endodermis. This localized auxin accumulation triggers an auxin signalling response in the endodermis, unleashing the active accommodation of the endodermis to the outgrowing LR. Essential in this process is the mechanical tension in the periclinal interface between the founder cells and the endodermis, which plays a key role in coordinating growth and auxin distribution. Root curvature promotes the initiation of LR (37, 38). According to our model, it would also increase tension on the periclinal interface between founder cells and endodermis, further promoting the redirection of the auxin flow toward the endodermis to trigger further radial expansion.

Bending stiffness of the endodermis limits the radial expansion of the pericycle. We investigated the mechanical factors influencing the expansion of activated XPP cells during lateral root initiation, considering the modest radial expansion induced by initial auxin-driven stress relaxation. We systematically analyzed the impact of various parameters on cell expansion, including the stiffness (E_0) and bending modulus (k_b) of founder cells and overlying endodermal cell walls, as well as turgor pressures in the founder cells (T_{p}) and the overlying endodermis (T_{en}). Expansion was quantified by measuring the length of the anticlinal wall between the activated XPP cells.

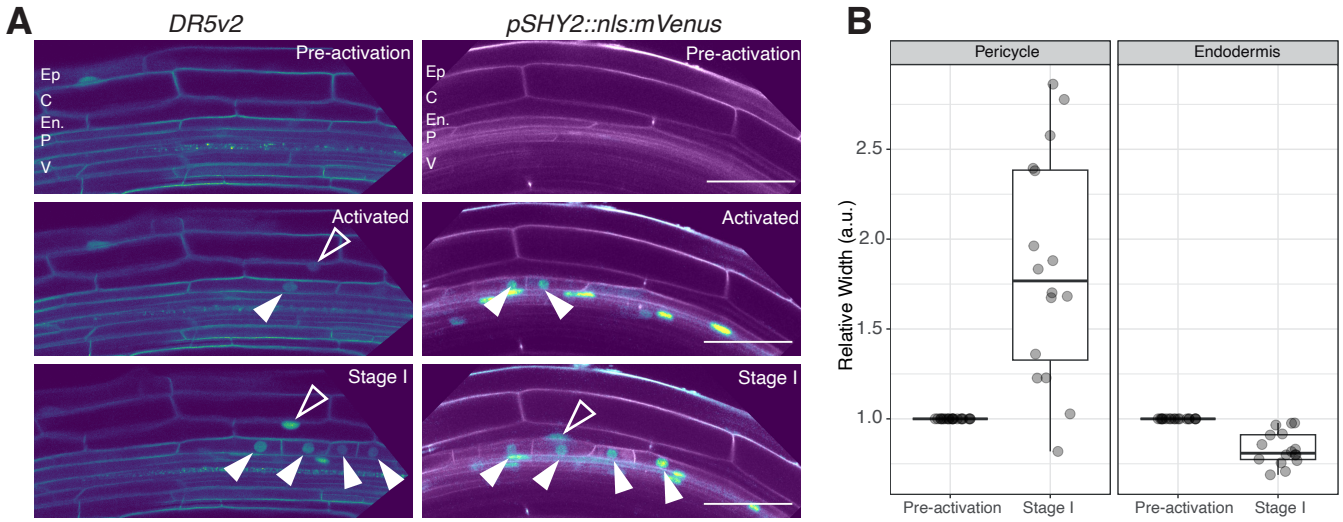

Fig. 3. Auxin signaling predates expression of SHY2 in the endodermis and endodermal accommodation. (A) Confocal sections of time-lapse recording monitoring the expression of auxin signalling (*DR5v2*) and *SHY2* expression ($pSHY2::nls:mVenus$) before pericycle activation, in founder cells and Stage I primordia. The filled arrowheads indicate a signal in the pericycle nuclei, and the open arrowheads signal in the endodermis. Note the *DR5v2* signal in the endodermis above the founder cells before the expression of *SHY2* in this tissue. The different layers are labelled vasculature (V), pericycle (P), endodermis (En), cortex (C) and epidermis (Ep). Of note, the cell outlines are labelled by the plasma membrane marker PIP4;1-GFP (for the *DR5v2* line) and by Propidium iodide (for the *pSHY2::nls:mVenus* line). Images are representative of three biological replicates. (B) Relative pericycle and endodermis cell width (measured at the junction between the two abutting pericycle cells) before activation and at Stage I. Values are for 16 measurements from five different roots before and after pericycle activation.

We found that reducing the bending modulus (k_b) from $3600\,\mathrm{MPa}$ to $100\,\mathrm{MPa}$ led to non-linear radial expansion, from 20% to 70%, resembling the trapezoidal morphology observed *in planta* (21, 23) (Fig. 4 A, E, F). An increase in pericycle turgor pressure (T_p), especially at very high values ($2\,\mathrm{MPa}$), amplified activated XPP cell expansion (Fig. 4 D). However, reductions in endodermal turgor (T_en) or elastic modulus (E_0) minimally affected pericycle expansion (Fig. 4 B, C). The contribution of the auxin transport to the outcome of these simulations was minor. Indeed, we ran simulations with maximum pericycle radial expansion conditions (endodermis k_b at $100\,\mathrm{MPa}$) with auxin transport enabled or disabled, which resulted in nearly identical founder cell expansion (Fig. S3).

These findings suggest that increased pericycle turgor and decreased endodermal resistance to deformation can enhance radial expansion. A notable difference between pericycle-turgor-driven and bending-modulus-driven radial expansion lies in the final shape of the founder cells. Upon turgor-driven expansion, the founder cells expanded less toward the endodermis, resulting in a flatter emerging lateral root primordium (LRP) tip. Combining higher pericycle turgor with lower endodermal turgor might rectify this directional bias deficiency. Auxin promotes the expression and activity of pumps and channels that contribute to water influx (39), which could contribute to a local increase of turgor pressure in the pericycle. However, this aspect must be mitigated by the quick water exchange that could lead to equilibration of the turgor pressure (40).

The reduction in the bending resistance of the endodermis wall facing the pericycle has the most important contribution to the founder cells expansion. What molecular process could modulate this bending resistance in vivo? Recent research highlighted the distinct organization of cortical microtubules (CMTs) in the endodermis, with an ordered longitudinally oriented array on the pericycle-facing side. LR initiation induces reorganization of these microtubules, involving auxin-dependent induction of the microtubule-associated protein MAP70-5 (34). CMTs influence wall mechanical properties through cellulose fibril deposition orientation control. MAP70-5 expression could alter CMTs and endodermal wall properties, enhancing founder cell expansion (Fig. S5). The organisation and/or dynamics of the CMTs arrays could thus be a modulator of the bending resistance of the endodermis. Supporting this view, abolishing completely the bending resistance (setting (k_b) to $0\,\mathrm{MPa}$) leads to a froth-like behaviour of the tissue (Fig. S5), reminiscent of the aspect of roots cells when treated with the CMT depolymerising agent oryzalin (41). The radial expansion of the shared anticlinal cell wall primarily occurs after the first anticlinal divisions of founder cells. As our model does not implement cell divisions, investigating how new anticlinal cell interfaces contribute to radial expansion could provide valuable insights.

Endodermis architecture defines LRP shape. We explored whether the arrangement of endodermis cells above the founder cells impacted pericycle growth and shape. Our simulations have mainly focused on lattices where two adjacent endodermal cells overlay the two activated XPP cells, resulting in one endodermis-endodermis interface above the pericycle. We simulated cases with either no endodermis-endodermis interface or two such interfaces overlying the pericycle. Employing the same parameters as before (bending modulus of both the FCs and overlying endodermal cells at $k_b = 100\mathrm{MPa}$), we present the outcomes (Fig. 4 H-J).

When only one endodermal cell overlays the pericycle, no

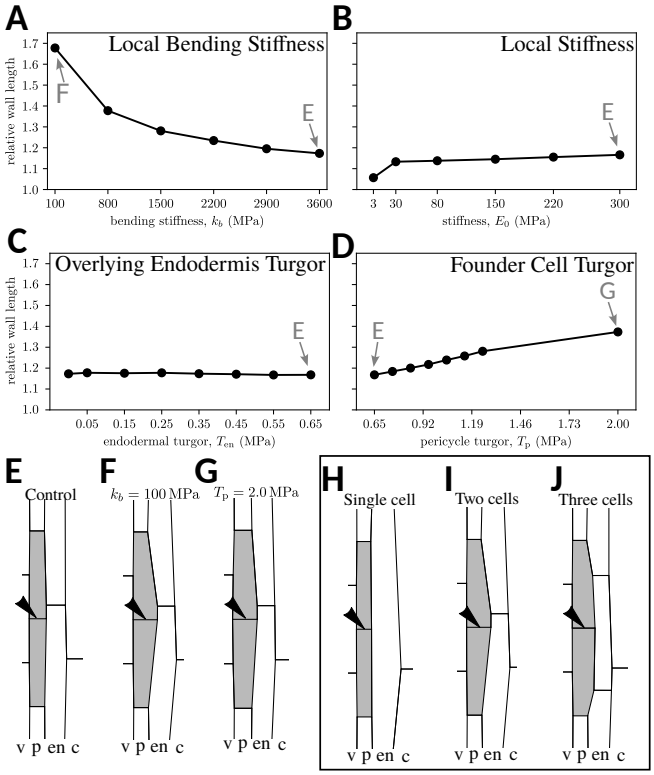

Fig. 4. The endodermis's mechanical properties, topology, and geometry potentiate radial expansion and define LRP shape. (A-D) Relative length of the shared wall between primed XPP cells (grey) for different values of the overlying endodermis and founder cell bending modulus (k_b, A), stiffness (E_0, B), overlying endodermis turgor (T_{en}, C) and founder cell turgor (T_p, D). (E-G) Morphology of the ends-state of the simulations. The grey arrows and letters in (A-D) indicate the corresponding morphologies in (E-G). (H-J) Growth simulation results with one (H), two (I), and three (J) endodermal cells overlying the activated XPP cells. The arrowheads indicate the shared wall between primed XPP cells. The labelled layers are vasculature (v), pericycle (p), endodermis (en), and cortex (c).

radial expansion was observed, as there was no strain on the endodermis-pericycle wall (Fig. 4 H). The reduced strain and stress on the wall between the activated XPP cells corresponded to a slower growth rate (Fig. S6 A). To rule out limited degrees of freedom as a causal factor, we conducted simulations where the endodermis-endodermis junction was removed while retaining the respective vertices for displacement. This also resulted in a lack of pericycle expansion (Fig. S6 B, C).

In contrast, the configuration with three overlying endodermal cells led to distinct results (Fig. 4 J). In this scenario, the founder cells expanded to a maximum width, similar to the earlier two-cell configuration (Fig. 4 I, J, Fig. S6 A). However, the resulting shape showed noticeable divergence, with the three-cell arrangement producing a flatter tip than the two-cell counterpart.

These findings suggest that the spatial arrangement of endodermis cells governs the shape of the developing primordium, and not all configurations equally support the radial expansion of the primed pericycle. A prior study tracking cell lineage in lateral root primordia consistently observed that the initial activated XPP cell division always occurred beneath an endodermal junction (42). Since radial expansion precedes activated XPP cell division (33), this observation underscores the critical role of endodermis topology. The dependence of lateral root primordium shape on endodermis topology complicates our understanding of LR initiation. The number and arrangement of overlying endodermal cells dictate the extent and direction of pericycle expansion. As additional founder cells are recruited laterally (32), the implications for LR morphogenesis and tissue morphology modulation during growth are intriguing, especially in a three-dimensional context not captured by our two-dimensional model.

Conclusions

Our study combines computational modelling and empirical observations to explore the mechanical bases governing the radial expansion of founder cells and endodermal accommodation during lateral root initiation. The central role of auxin in mediating growth and its subsequent impact on mechanical stress distribution emerge as critical components of this process. We find that the mechanical properties of the endodermis are pivotal in shaping the radial expansion of founder cells. Reducing the bending stiffness of endodermal cell walls significantly promotes pericycle growth, highlighting the mechanical regulation of cell expansion. This complements existing knowledge about the role of turgor pressure in growth and emphasizes the importance of localized modifications in cell wall properties for cell growth.

Material and methods

Plant material and growth. Seedlings of sC111 (*pUBQ10::GFP:PIP1; pGATA23::H2B:mcherry; pDR5v2::YFP:nls*) (33) and *pSHY2::nls:mVenus; pLBD16::mCherry:SYP122* (31) were used to monitor DR5v2 and SHY2/IAA3, respectively. Seeds were surface-sterilized with Ethanol 70% and SDS 0.05% for $5\,\mathrm{min}$, rinsed once with ethanol 99% and air-dried. After stratification at $4°$C for $48\,\mathrm{h}$, seedlings were grown vertically on square Petri dishes plates containing Murashige and Skoog $0.5\times$ medium with a pH of 5.7, 0.8% agar and 1% sucrose, at $22°$C with a photoperiod of $8/16\,\mathrm{h}$ light/dark condition. Four days after germination, lateral root primordium (LRP) induction through $5\,\mathrm{h}$ of gravistimulation (turned plates vertically, $180°$) to detect early events of LRP formation was applied and to proceed with live imaging.

Live Imaging and Microscopy. For imaging, the seedlings were transferred to a chambered cover glass as described in (43), Propidium Iodide ($2\,\mu\mathrm{g/mL}$) was added when required, and Confocal Laser-Scanning Microscopy (CLSM) was performed on a Leica SP8 confocal microscope with a $63\times$, NA = 1.2 water immersion objective. GFP, YFP and mVenus fluorescence were detected using the $488\,\mathrm{nm}$ and $514\,\mathrm{nm}$ excitation laser line and a detection range of 495-$560\,\mathrm{nm}$ and 524-$550\,\mathrm{nm}$, respectively. mCherry and Propidium Iodide fluorescence was detected using the 568 nm excitation laser line and a detection range of 590-$750\,\mathrm{nm}$. Images were taken every $30\,\mathrm{min}$ after LRP induction for $\sim 12\,\mathrm{h}$ with a resolution of 1024×1024 pixels, $400\,\mathrm{Hz}$ speed and a line average of 4.

Z stacks were performed using a z-step size of 0.5mm. Post-processing of images (LUT, Bright, contrast and maximum intensity projections of 3-7 z-sections was performed in Fiji (http://fiji.sc/Fiji)).

ACKNOWLEDGEMENTS
We thank J. Dubrovsky and J. Vermeer for their critical comments on the manuscript.

COMPETING FINANCIAL INTERESTS
The authors declare no competing or financial interests.

AUTHOR CONTRIBUTIONS
Conceptualization: J. Ramos, K. Alim, A. Maizel; Methodology: J. Ramos, K. Alim; Formal analysis: J. Ramos, K. Alim; Investigation: J. Ramos, B. Reyes-Hernández; Data curation: J. Ramos, B. Reyes-Hernández; Writing-original draft: J. Ramos, A. Maizel; Writing-review & editing: J. Ramos, K. Alim, A. Maizel; Visualization: J. Ramos, B. Reyes-Hernández ; Supervision: K. Alim, A. Maizel; Funding acquisition: K. Alim, A. Maizel

FUNDING
This work was supported by the German Research Foundation (DFG) through the FOR2581 grants (MA5293/6-2, AL1429/4-1 and AL1429/3-1) and the Consejo Nacional de Ciencia y Tecnología of Mexico (CONACYT) to BJRH (grant 740701).

SUPPORTING INFORMATION
Supplementary information is available online at: XXXXXX

PEER REVIEW HISTORY
The peer review history is available online at: XXXXXX

Bibliography

1. Christopher D. Whitewoods, Beatriz Gonçalves, Jie Cheng, Minlong Cui, Richard Kennaway, Karen Lee, Claire Bushell, Man Yu, Chunlan Piao, and Enrico Coen. Evolution of carnivorous traps from planar leaves through simple shifts in gene expression. *Science*, 367(6473):91–96, 2020. doi: 10.1126/science.aay5433.
2. Takahiro Yamaguchi, Hirokazu Tsukaya, Hironori Fujita, Kenji Fukushima, Mitsuyasu Hasebe, and Masayoshi Kawaguchi. Oriented cell division shapes carnivorous pitcher leaves of Sarracenia purpurea. *Nature Communications*, 6(1):1–10, 2015. doi: 10.1038/ncomms7450.
3. Zhaojun Ding and Jiří Friml. Auxin regulates distal stem cell differentiation in *Arabidopsis* roots. *Proceedings of the National Academy of Sciences*, 107(26):12046–12051, 2010. doi: 10.1073/pnas.1000672107.
4. Ottoline Leyser. Auxin Signaling. *Plant Physiology*, 176(1):465–479, jan 2018. ISSN 0032-0889. doi: 10.1104/pp.17.00765.
5. William D. Teale, Ivan A. Paponov, and Klaus Palme. Auxin in action: signalling, transport and the control of plant growth and development. *Nature Reviews Molecular Cell Biology*, 7 (11):847–859, nov 2006. ISSN 1471-0072. doi: 10.1038/nrm2020.
6. Jodi L Stewart and Jennifer L Nemhauser. Do Trees Grow on Money? Auxin as the Currency of the Cellular Economy. *Cold Spring Harbor Perspectives in Biology*, 2(2):a001420–a001420, feb 2010. ISSN 1943-0264. doi: 10.1101/cshperspect.a001420.
7. Didier Reinhardt, Eva-Rachele Pesce, Pia Stieger, Therese Mandel, Kurt Baltensperger, Malcolm Bennett, Jan Traas, Jiří Friml, and Cris Kuhlemeier. Regulation of phyllotaxis by polar auxin transport. *Nature*, 426(6964):255–60, 2003. ISSN 1476-4687. doi: 10.1038/nature02081.
8. Teva Vernoux, Fabrice Besnard, and Jan Traas. Auxin at the Shoot Apical Meristem. *Cold Spring Harbor Perspectives in Biology*, 2(4):a001487–a001487, apr 2010. ISSN 1943-0264. doi: 10.1101/cshperspect.a001487.
9. Massimiliano Sassi and Teva Vernoux. Auxin and self-organization at the shoot apical meristem. *Journal of Experimental Botany*, 64(9):2579–2592, jun 2013. ISSN 1460-2431. doi: 10.1093/jxb/ert101.
10. Siobhan A. Braybrook and Alexis Peaucelle. Mechano-Chemical Aspects of Organ Formation in Arabidopsis thaliana: The Relationship between Auxin and Pectin. *PLoS ONE*, 8(3): e57813, mar 2013. ISSN 1932-6203. doi: 10.1371/journal.pone.0057813.
11. Alexis Peaucelle, Siobhan A. Braybrook, Laurent Le Guillou, Emeric Bron, Cris Kuhlemeier, and Herman Höfte. Pectin-Induced Changes in Cell Wall Mechanics Underlie Organ Initiation in Arabidopsis. *Current Biology*, 21(20):1720–1726, oct 2011. ISSN 09609822. doi: 10.1016/j.cub.2011.08.057.
12. J. Petrasek and J. Friml. Auxin transport routes in plant development. *Development*, 136 (16):2675–2688, aug 2009. ISSN 0950-1991. doi: 10.1242/dev.030353.
13. Eric M. Kramer and Malcolm J. Bennett. Auxin transport: a field in flux. *Trends in Plant Science*, 11(8):382–386, aug 2006. ISSN 13601385. doi: 10.1016/j.tplants.2006.06.002.
14. Richard S Smith. The Role of Auxin Transport in Plant Patterning Mechanisms. *PLoS Biology*, 6(12):e323, dec 2008. ISSN 1545-7885. doi: 10.1371/journal.pbio.0060323.
15. Didier Reinhardt, Therese Mandel, and Cris Kuhlemeier. Auxin Regulates the Initiation and Radial Position of Plant Lateral Organs. *The Plant Cell*, 12(4):507, apr 2000. ISSN 10404651. doi: 10.2307/3871065.
16. Richard S Smith, S. Guyomarc'h, Therese Mandel, Didier Reinhardt, Cris Kuhlemeier, and Przemyslaw Prusinkiewicz. A plausible model of phyllotaxis. *Proceedings of the National Academy of Sciences USA*, 103(5):1301–1306, jan 2006. ISSN 0027-8424. doi: 10.1073/pnas.0510457103.
17. Neha Bhatia, Behruz Bozorg, André Larsson, Carolyn Ohno, Henrik Jönsson, and Marcus G. Heisler. Auxin Acts through MONOPTEROS to Regulate Plant Cell Polarity and Pattern Phyllotaxis. *Current Biology*, 26(23):3202–3208, dec 2016. ISSN 09609822. doi: 10.1016/j.cub.2016.09.044.
18. Marcus G. Heisler, Olivier Hamant, Pawel Krupinski, Magalie Uyttewaal, Carolyn Ohno, Henrik Jönsson, Jan Traas, and Elliot M. Meyerowitz. Alignment between PIN1 Polarity and Microtubule Orientation in the Shoot Apical Meristem Reveals a Tight Coupling between Morphogenesis and Auxin Transport. *PLoS Biology*, 8(10):e1000516, oct 2010. ISSN 1545-7885. doi: 10.1371/journal.pbio.1000516.
19. Naomi Nakayama, Richard S Smith, Therese Mandel, Sarah Robinson, Seisuke Kimura, Arezki Boudaoud, and Cris Kuhlemeier. Mechanical regulation of auxin-mediated growth. *Current Biology*, 22(16):1468–1476, August 2012.
20. D. Ramos, João R., Maizel, Alexis, and Alim, Karen. Tissue-wide integration of mechanical cues promotes effective auxin patterning. *Eur. Phys. J. Plus*, 136(2):250, 2021. doi: 10.1140/epjp/s13360-021-01204-6.
21. Amaya Vilches-Barro and Alexis Maizel. Talking through walls: Mechanisms of lateral root emergence in Arabidopsis thaliana. *Current Opinion in Plant Biology*, 23(May):31–38, 2015. ISSN 13695266. doi: 10.1016/j.pbi.2014.10.005.
22. Dorothee Stoeckle, Martha Thellmann, and Joop EM Vermeer. Breakout — lateral root emergence in Arabidopsis thaliana. *Current Opinion in Plant Biology*, 41:67–72, feb 2018. ISSN 13695266. doi: 10.1016/j.pbi.2017.09.005.
23. Yujuan Du and Ben Scheres. Lateral root formation and the multiple roles of auxin. *Journal of Experimental Botany*, 69(2):155–167, 07 2017. ISSN 0022-0957. doi: 10.1093/jxb/erx223.
24. Joseph G. Dubrovsky, Michael Sauer, Selene Napsucialy-Mendivil, Maria G. Ivanchenko, Jiří Friml, Svetlana Shishkova, John Celenza, and E. Benkova. Auxin acts as a local morphogenetic trigger to specify lateral root founder cells. *Proceedings of the National Academy of Sciences USA*, 105(25):8790–8794, jun 2008. ISSN 0027-8424. doi: 10.1073/pnas.0712307105.
25. Eva Benková, Marta Michniewicz, Michael Sauer, Thomas Teichmann, Daniela Seifertová, Gerd Jürgens, and Jiřı Friml. Local, Efflux-Dependent Auxin Gradients as a Common Module for Plant Organ Formation. *Cell*, 115(5):591–602, nov 2003. ISSN 00928674. doi: 10.1016/S0092-8674(03)00924-3.
26. Anna N. Stepanova, Joyce Robertson-Hoyt, Jeonga Yun, Larissa M. Benavente, De-Yu Xie, Karel Doležal, Alexandra Schlereth, Gerd Jürgens, and Jose M. Alonso. *TAA1*-mediated auxin biosynthesis is essential for hormone crosstalk and plant development. *Cell*, 133(1): 177–191, Apr 2008. ISSN 0092-8674. doi: 10.1016/j.cell.2008.01.047.
27. Alan Marchant, Rishikesh Bhalerao, Ilda Casimiro, Jan Eklöf, Pedro J. Casero, Malcolm Bennett, and Goran Sandberg. AUX1 Promotes Lateral Root Formation by Facilitating Indole-3-Acetic Acid Distribution between Sink and Source Tissues in the Arabidopsis Seedling. *The Plant Cell*, 14(3):589–597, mar 2002. ISSN 1040-4651. doi: 10.1105/tpc.010354.
28. Kamal Swarup, Eva Benková, Ranjan Swarup, Ilda Casimiro, Benjamin Péret, Yaodong Yang, Geraint Parry, Erik Nielsen, Ive De Smet, Steffen Vanneste, Mitch P. Levesque, David Carrier, Nicholas James, Vanessa Calvo, Karin Ljung, Eric Kramer, Rebecca Roberts, Neil Graham, Sylvestre Marillonnet, Kanu Patel, Jonathan D.G. Jones, Christopher G. Taylor, Daniel P. Schachtman, Sean May, Goran Sandberg, Philip Benfey, Jiri Friml, Ian Kerr, Tom Beeckman, Laurent Laplaze, and Malcolm J. Bennett. The auxin influx carrier LAX3 promotes lateral root emergence. *Nature Cell Biology*, 10(8):946–954, aug 2008. ISSN 1465-7392. doi: 10.1038/ncb1754.
29. B. Péret, A. M. Middleton, A. P. French, A. Larrieu, A. Bishopp, M. Njo, D. M. Wells, S. Porco, N. Mellor, L. R. Band, I. Casimiro, J. Kleine-Vehn, S. Vanneste, I. Sairanen, R. Mallet, G. Sandberg, K. Ljung, T. Beeckman, E. Benková, J. Friml, E. Kramer, J. R. King, I. De Smet, T. Pridmore, M. Owen, and M. J. Bennett. Sequential induction of auxin efflux and influx carriers regulates lateral root emergence. *Molecular Systems Biology*, 9(1):699–699, apr 2014. ISSN 1744-4292. doi: 10.1038/msb.2013.43.
30. Peter Marhavý, Marleen Vanstraelen, Bert De Rybel, Ding Zhaojun, Malcolm J. Bennett, Tom Beeckman, and Eva Benková. Auxin reflux between the endodermis and pericycle promotes lateral root initiation. *The EMBO Journal*, 32(1):149–158, nov 2012. ISSN 0261-4189. doi: 10.1038/emboj.2012.303.
31. J. E. M. Vermeer, D. von Wangenheim, M. Barberon, Y. Lee, E. H. K. Stelzer, A. Maizel, and N. Geldner. A Spatial Accommodation by Neighboring Cells Is Required for Organ Initiation in Arabidopsis. *Science*, 343(6167):178–183, jan 2014. ISSN 0036-8075. doi: 10.1126/science.1245871.
32. Héctor H Torres-Martínez, Paul Hernández-Herrera, Gabriel Corkidi, and Joseph G Dubrovsky. From one cell to many: Morphogenetic field of lateral root founder cells in arabidopsis thaliana is built by gradual recruitment. *Proceedings of the National Academy of Sciences*, 117(34):20943–20949, August 2020.
33. Amaya Vilches Barro, Dorothee Stöckle, Martha Thellmann, Paola Ruiz-Duarte, Lotte Bald, Marion Louveaux, Patrick von Born, Philipp Denninger, Tatsuaki Goh, Hidehiro Fukaki, Joop E.M. Vermeer, and Alexis Maizel. Cytoskeleton dynamics are necessary for early events of lateral root initiation in arabidopsis. *Current Biology*, 29(15):2443–2454.e5, August 2019. doi: 10.1016/j.cub.2019.06.039.
34. Dorothee Stöckle, Blanca Jazmin Reyes-Hernández, Amaya Vilches Barro, Milica Nenadić, Zsofiá Winter, Sophie Marc-Martin, Lotte Bald, Robertas Ursache, Satoshi Fujita, Alexis Maizel, and Joop EM Vermeer. Microtubule-based perception of mechanical conflicts controls plant organ morphogenesis. *Science Advances*, 8(6):eabm4974, 2022. doi: 10.1126/sciadv.abm4974.
35. Qing Tian, Nicholas J. Uhlir, and Jason W. Reed. Arabidopsis SHY2/IAA3 Inhibits Auxin-Regulated Gene Expression . *The Plant Cell*, 14(2):301–319, 02 2002. ISSN 1040-4651. doi: 10.1105/tpc.010283.
36. D.R. Boer, A. Freire Rios, W.A.M. van den Berg, T. Saaki, I.W. Manfield, S. Kepinski, I. López-Vidrieo, J.M. Franco-Zorilla, S.C. de Vries, R. Solano, D. Weijers, and M. Coll. Structural basis for dna binding specificity by the auxin-dependent arf transcription factors. *Cell*, 156:577–589, 2014. ISSN 0092-8674. doi: 10.1016/j.cell.2013.12.027.
37. Stefan Kircher and Peter Schopfer. Priming and positioning of lateral roots in Arabidopsis. An approach for an integrating concept. *Journal of Experimental Botany*, 67(5):1411–1420, 12 2015. ISSN 0022-0957. doi: 10.1093/jxb/erv541.

38. Marta Laskowski, Verônica A Grieneisen, Hugo Hofhuis, Colette A. ten Hove, Paulien Hogeweg, Athanasius F. M Marée, and Ben Scheres. Root system architecture from coupling cell shape to auxin transport. *PLOS Biology*, 6(12):1–15, 12 2008. doi: 10.1371/journal.pbio.0060307.
39. Katrin Philippar, Natalya Ivashikina, Peter Ache, May Christian, Hartwig Lüthen, Klaus Palme, and Rainer Hedrich. Auxin activates kat1 and kat2, two k+-channel genes expressed in seedlings of arabidopsis thaliana. *The Plant Journal*, 37(6):815–827, 2004. doi: https://doi.org/10.1111/j.1365-313X.2003.02006.x.
40. Yoselin Benitez-Alfonso, Christine Faulkner, Ali Pendle, Shunsuke Miyashima, Ykä Helariutta, and Andrew Maule. Symplastic Intercellular Connectivity Regulates Lateral Root Patterning. *Developmental Cell*, 26(2):136–147, jul 2013. ISSN 15345807. doi: 10.1016/j.devcel.2013.06.010.
41. Tobias I. Baskin, Gerrit T.S. Beemster, Jan E. Judy-March, and Francoise Marga. Disorganization of Cortical Microtubules Stimulates Tangential Expansion and Reduces the Uniformity of Cellulose Microfibril Alignment among Cells in the Root of Arabidopsis. *Plant Physiology*, 135(4):2279–2290, 08 2004. ISSN 0032-0889. doi: 10.1104/pp.104.040493.
42. Daniel von Wangenheim, Jens Fangerau, Alexander Schmitz, Richard S Smith, Heike Leitte, Ernst H K Stelzer, and Alexis Maizel. Rules and Self-Organizing properties of post-embryonic plant organ cell division patterns. *Curr. Biol.*, 26(4):439–449, January 2016.
43. Peter Marhavý and Eva Benková. Real-time analysis of lateral root organogenesis in arabidopsis. *Bio Protoc*, 5(8), April 2015.

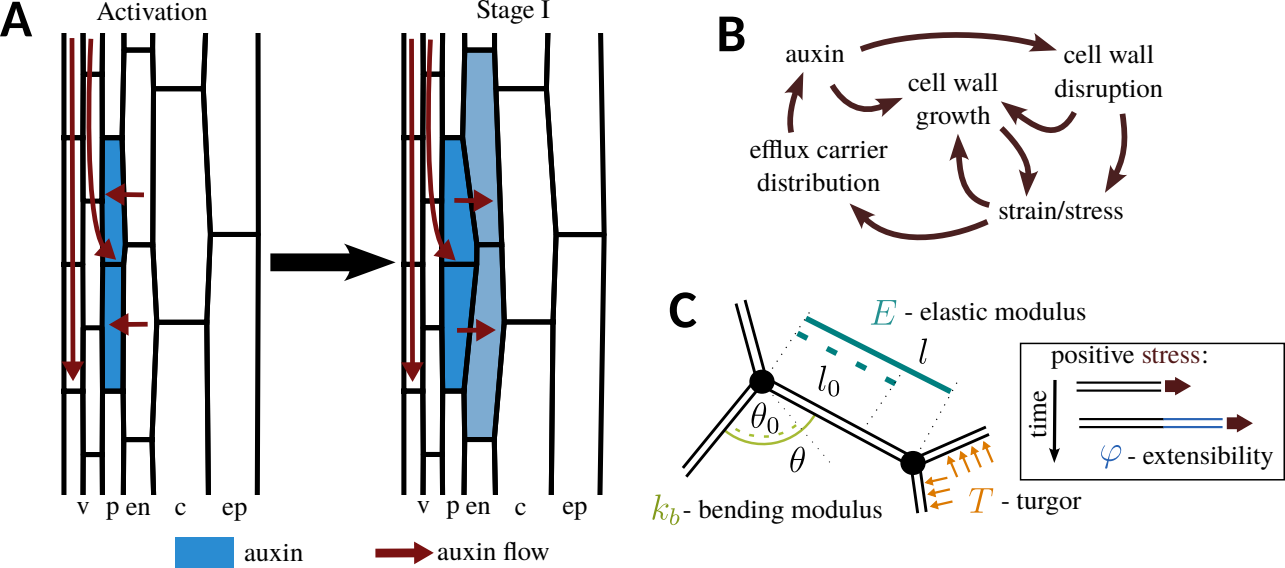
A
Activation
Stage I
v
p
en
c
ep
auxin
auxin flow
B
auxin
cell wall
disruption
cell wall
growth
efflux carrier
distribution
strain/stress
C
E - elastic modulus
l
l_0
θ_0
θ
k_b - bending modulus
T - turgor
positive stress:
time
φ - extensibility

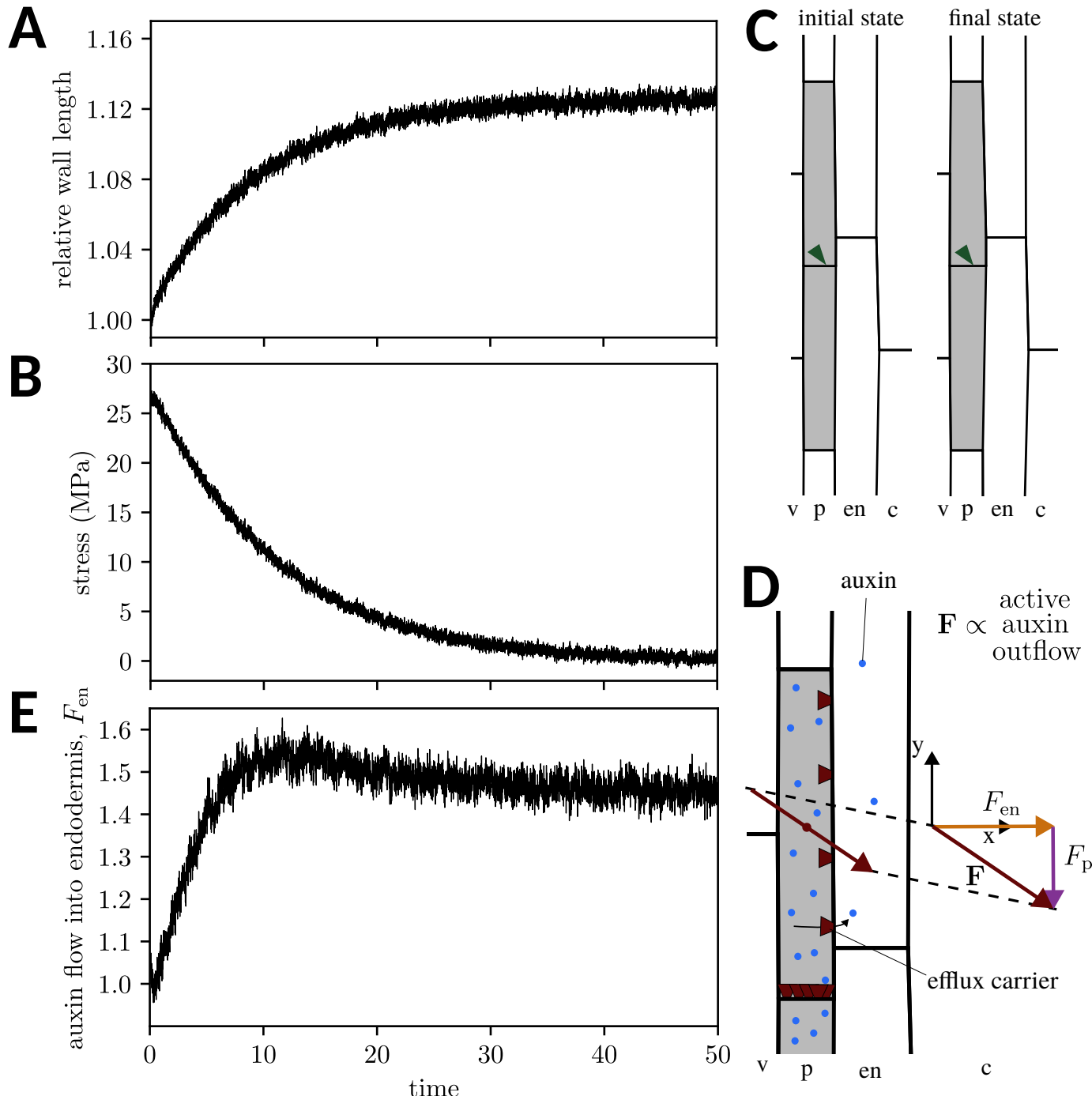
A
relative wall length
1.16
1.12
1.08
1.04
1.00
B
stress (MPa)
30
25
20
15
10
5
0
E
auxin flow into endodermis, F_{en}
1.6
1.5
1.4
1.3
1.2
1.1
1.0
0
10
20
30
40
50
time
C
initial state
final state
v p en c
v p en c
D
auxin
$\mathbf{F} \propto$ active auxin outflow
y
x
F_{en}
F_p
$\mathbf{F}$
efflux carrier
v p en c

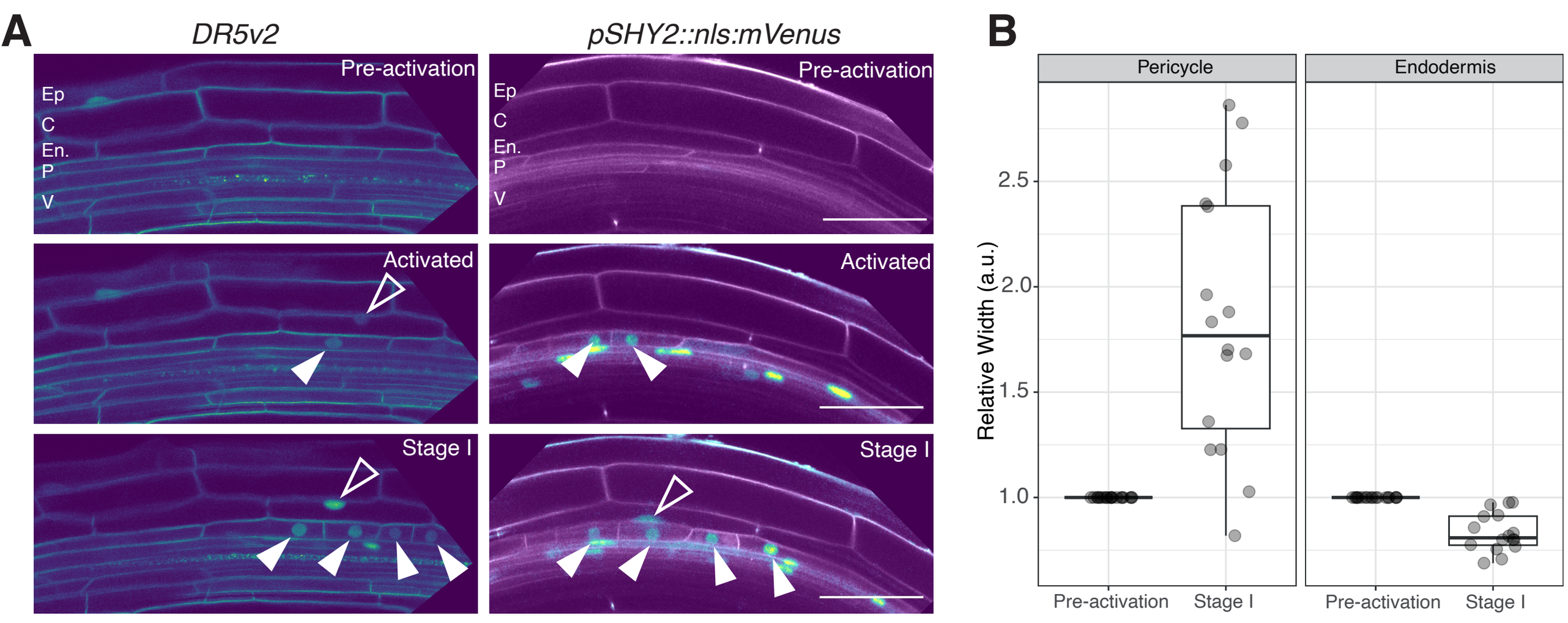
A
DR5v2
pSHY2::nls:mVenus
Pre-activation
Ep
C
En.
P
V
Activated
Stage I
B
Pericycle
Endodermis
Relative Width (a.u.)
2.5
2.0
1.5
1.0
Pre-activation
Stage I

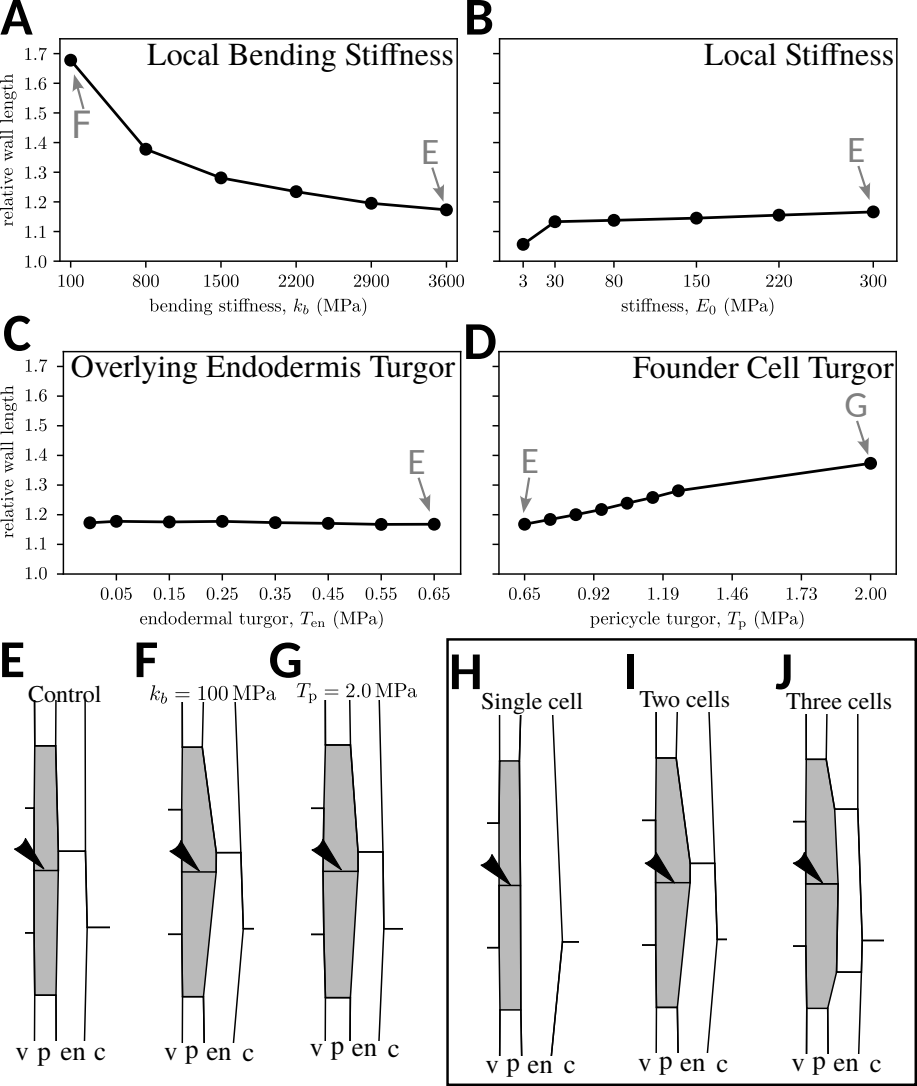
A
Local Bending Stiffness
relative wall length
1.7
1.6
1.5
1.4
1.3
1.2
1.1
1.0
F
E
100
800
1500
2200
2900
3600
bending stiffness, k_b (MPa)
B
Local Stiffness
E
3
30
80
150
220
300
stiffness, E_0 (MPa)
C
Overlying Endodermis Turgor
relative wall length
E
0.05
0.15
0.25
0.35
0.45
0.55
0.65
endodermal turgor, T_{en} (MPa)
D
Founder Cell Turgor
G
E
0.65
0.92
1.19
1.46
1.73
2.00
pericycle turgor, T_{p} (MPa)
E
Control
F
$k_b = 100\,\mathrm{MPa}$
G
$T_{\mathrm{p}} = 2.0\,\mathrm{MPa}$
v p en c
v p en c
v p en c
H
Single cell
I
Two cells
J
Three cells
v p en c
v p en c
v p en c